Retrieving Temperatures and Single Scattering Albedos from Martian Spectral Data Using Neural Networks.
L. He[1], R. E. Arvidson[2], D. V. Politte[2], T. Condus[2] and J. A. O'Sullivan[1]. [1]Department of Electrical and Systems Engineering, Washington University in St. Louis, Saint Louis, MO, [2]Department of Earth and Planetary Sciences, Washington University in St. Louis, Saint Louis, MO.

Introduction: In this abstract we present the use of a machine learning neural network approach, Separating Temperature and Albedo by Neural Networks (STANN), to retrieve both surface single scattering albedos (SSA) and kinetic temperatures (*T*) using CRISM hyperspectral imaging data as an example application. The issue is that the retrieval of both SSA and T from emission spectra at thermal wavelengths (e.g., THEMIS and TES), and from mixed solar and thermal wavelengths (e.g., CRISM and OMEGA), is an underdetermined and ill-posed problem. We use the pipeline processing developed by us over the past few years to model atmospheric effects (gases and aerosols) with DISORT [1] and the Hapke function [2] for surface scattering and emission, followed by application of a log maximum likelihood approach to retrieve denoised and sharpened SSA spectra and images [3]. We now show how to retrieve both solar and thermal effects in this pipeline using a neural network approach, using Mars Reconnaissance Orbiter CRISM scene FRT0000B6F1 covering Mount Sharp as an example. In a companion abstract Condus et al. [4] show application of our pipeline to THEMIS and TES data.

Mathematical Model: We use the function *f* to describe our overall approach. For the j^{th} band whose wavelength is λ_j, the radiance at this band r_j can be computed based on the surface temperature *T*, the spatial geometric information *l*, and the single scattering albedo s_j as

$$r_j = f(s_j, T, l, \lambda_j).$$

To retrieve the SSA and the temperature, we need to find the inverse function as

$$[s_j, T] = f^{-1}(r_j, l, \lambda_j).$$

The difficulty of approximating this inverse function by a neural network depends on properties of the function *f*. We quantify this difficulty by defining the sensitivity Δr of *f* with respect to the temperature as

$$\Delta r = \frac{f(s^*, T+\Delta T, l^*, \lambda) - f(s^*, T, l^*, \lambda)}{\Delta T}$$, which is plotted in Fig. 1. Warmer temperatures lead to higher sensitivities and better retrievals.

Framework: Fig. 2 shows how STANN works in general. The scene spectral radiance cube and corresponding incidence, emergence and phase angles for each pixel, together with a DISORT-generated look-up table are inputs. The output is a retrieved temperature map and the corresponding SSA spectral cube.

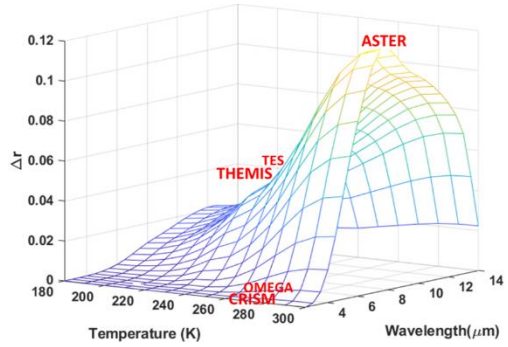

Fig. 1. The sensitivity for instruments quoted in Table 1 above for an SSA of 0.6, for incidence, emergence, and phase angles of 1.62, 82.91 and 108.79 degrees respectively. ASTER is shown for comparison to Mars environmental conditions, i.e., surface kinetic temperatures.

Table 1. Wavelength coverage for relevant Mars spectrometers and ASTER on the Earth Observing System.

Spectrometer	Planet	Spectral (μm)
Compact Imaging Spectrometer for Mars (CRISM) [5]	Mars	0.4-3.9
Observatoire pour la Minéralogie, l'Eau, les Glaces et l'Activité (OMEGA) [6]	Mars	0.5-5.2
Mars Odyssey Thermal Emission Imaging System (THEMIS) [7]	Mars	6.8-14.9
Thermal Emission Spectrometer (TES) [8]	Mars	6-50
Advanced Spaceborne Thermal Emission and Reflection Radiometer (ASTER)	Earth	0.5-11.7

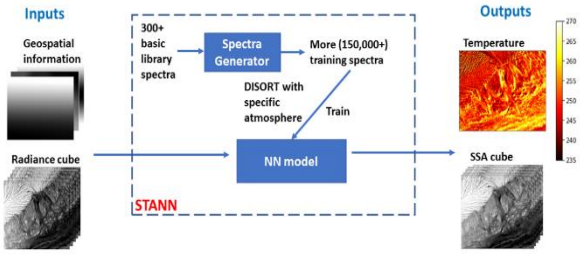

Fig. 2. Framework for STANN. CRISM FRT0000B6F1 scene is used as an example.

In the following, we show the application of the method to CRISM scene FRT0000B6F1 over Gale Crater.

Neural Network. We use a one-layer neural network to separate the temperatures and single scattering albedo spectra for CRISM data on a pixel by pixel basis (Fig. 3). The activation function is chosen as reLU and is defined as $g(x)=\max(0,x)$ for all hidden nodes. Both SSA inputs and outputs are scaled to the range [0,1]. To train

the NN we estimate the SSA spectra and temperature using Mars-relevant laboratory spectra and a random temperature map generated from DISORT-based simulations for each spatial pixel m and compare these to input values. We use a backpropagation method to minimize the sums of squares of deviations between actual and predicted values. An L-2 norm regularization is used to avoid overfitting and the regularization weight is chosen by cross validation.

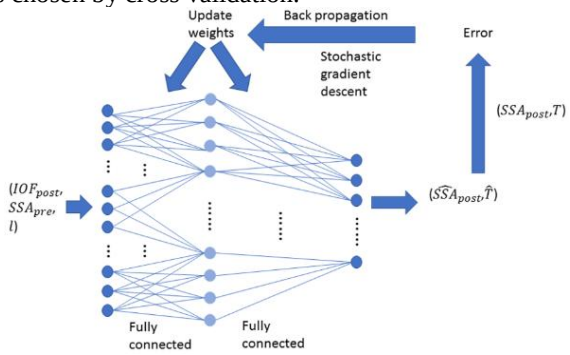

Fig. 3. Neural network model for CRISM and its backward training process using simulated data.

Training Set Generator. A key issue is the sensitivity of retrievals to the number of training spectra employed. Mao et al. used a 2-layer neural network with 800 hidden nodes for each layer, but trained it on less than 8000 samples [9]. Fig. 4 shows how our performance changes over the number of training samples. A large number of spectra are needed to guarantee that the network is well trained (at least 150,000). We thus generate a large number of laboratory spectra using various techniques, including a linear generator, simple autoencoder, variational autoencoder and generative adversarial networks, and compare the fidelity of the retrievals from actual data.

Performance: CRISM FRT000B6F1 was acquired on 2008-07-09T09, 15:29 LTST, 96.3˚ Ls. This scene covers the northern part Mount Sharp and includes Curiosity's traverse locations (Fig. 5). Curiosity's REMS instrument [10] measured the diurnal surface temperatures at the same LTST and season (corresponding to sols 1891, 1892) as acquisition of the CRISM scene, although necessarily after the rover's landing in 2012. The REMS temperature for CRISM's LTST is 242 K whereas we estimate for this location from the CRISM data a mean of 246 K for a single pixel. Additional validation is proceeding by computation of a thermal model that covers the CRISM scene. Additional tests with scenes that overlap this scene are also underway.

References: [1] Stamnes K. et al. (1988) *Applied Optics, 27,* 2502–2509. [2] Hapke B. (2012) *Cambridge University Press.* [3] Kreisch C. D. et al. (2017) *Icarus, 282,* 136-151. [4] Condus T. et al. (2019) *LPSC.* [5] Murchie S. et al. (2007) *J. Geophys. Res.-Planets,* 112.E5. [6] Bibring J.-P. et al. (2004) *Mars Express: The Scientific Payload,*1240, 37-49. [7] Christensen P. R. et al. (2004) *Space Science Reviews 110, 85-130.* [8] Christensen P. R. et al. (2001) *J. Geophy. Res.-Planets,* 106, 23823-23871. [9] Mao K. et al. (2008) *IEEE Trans. Geo. and Remote Sensing,* 46, 200-208. [10] Gómez-Elvira J. et al. (2014) *J. Geophys.Res.-Planets* 119, 1680-1688.

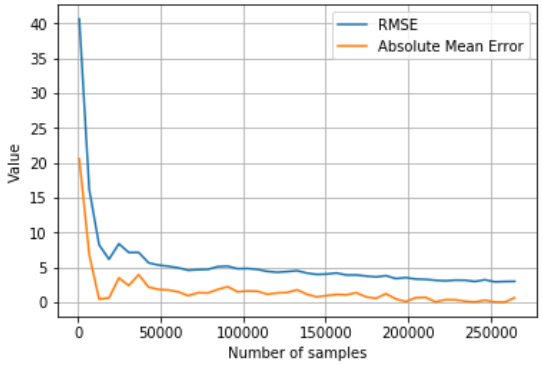

Fig. 4. Performance of our neural network for CRISM based on different training set sizes.

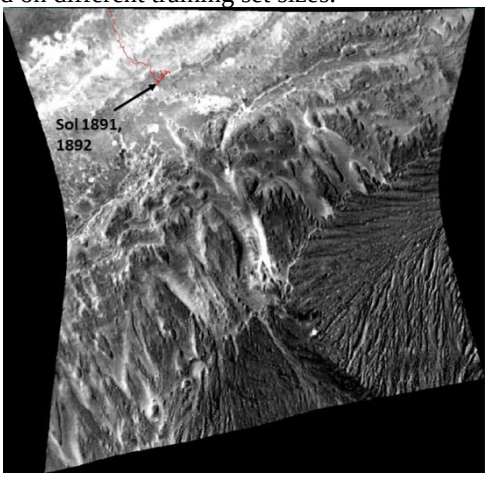

Fig. 5. Retrieved temperature map from CRISM data. The red curve shows Curiosity's traverses and sols 1891, 1892 location for REMS measurements.

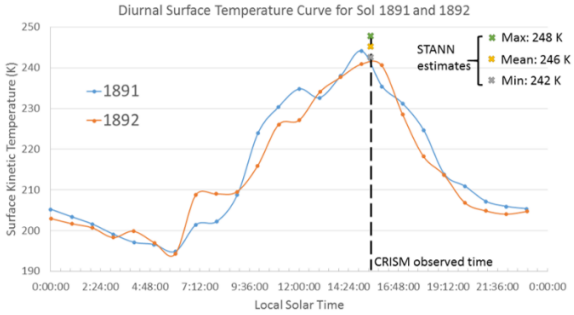

Fig. 6. Diurnal temperatures from REMS compared to the temperature retrieved from CRISM data.